



Loss of histone deacetylase Hdac1 disrupts metabolic processes in intestinal epithelial cells



Alexis Gonneaud, Naomie Turgeon, François-Michel Boisvert, François Boudreau, Claude Asselin *

Département d'anatomie et biologie cellulaire, Faculté de médecine et des sciences de la santé, Pavillon de recherche appliquée sur le cancer, Université de Sherbrooke, Sherbrooke, Québec J1E 4K8, Canada

ARTICLE INFO

Article history:

Received 17 July 2015

Accepted 7 August 2015

Available online 20 August 2015

Edited by Laszlo Nagy

Keywords:

Hdac1

Mitochondria

Reactive oxygen species

AMPK

Intestinal epithelial cell

Acetylation

ABSTRACT

By using acetyl-CoA as a substrate, acetyltransferases and histone deacetylases regulate protein acetylation by adding or removing an acetyl group on lysines. Nuclear-located Hdac1 is a regulator of intestinal homeostasis. We have previously shown that Hdac1 define specific intestinal epithelial cell basal and inflammatory-dependent gene expression patterns and control cell proliferation. We show here that Hdac1 depletion *in cellulo* leads to increased histone acetylation after metabolic stresses, and to metabolic disturbances resulting in impaired responses to oxidative stresses, AMPK kinase activation and mitochondrial biogenesis. Thus, nuclear Hdac1 may control intestinal epithelial cell metabolism by regulating the supply of acetyl groups.

© 2015 Federation of European Biochemical Societies. Published by Elsevier B.V. All rights reserved.

1. Introduction

Protein acetylation is a major post-translational modification regulated by acetyltransferases and deacetylases (HDAC), which respectively add or remove an acetyl group on lysine residues [1]. In addition to histones, many nuclear, cytoplasmic and mitochondrial proteins are acetylated, forming the acetylome [2]. Acetylation of histones relaxes DNA-histone interactions and creates binding sites for bromodomain-containing proteins, which affect chromatin structure and gene expression [1]. Acetylation of non-histone proteins modifies protein functions by altering protein interactions with other proteins or DNA, as well as protein stability and location [3,4]. Protein acetylation is a highly regulated process dependent on cell metabolites. Indeed, protein acetylation levels are dependent in part on the regulation of HDAC activity by endogenous HDAC inhibitors such as sphingosine-1-phosphate [5], β -hydroxybutyrate [6,7] and carnitine [8], whose levels vary with cell metabolism. Furthermore, histone acetylation depends on the availability of the substrate acetyl-CoA in nuclear and cytoplasmic compartments [9,10]. For example, citrate produced from glucose metabolism, through the Krebs cycle, is used by the ATP-citrate lyase (ACL) for acetyl-CoA production. ACL depletion leads to both reduced acetyl-CoA cellular levels and histone acetylation

[10]. Thus, cell energy-dependent variations of acetyl-CoA levels or HDAC-inhibiting metabolites may lead to alterations in the acetylome as well as epigenetic signalling.

Members of the HDAC family are divided in three classes, including nuclear class I enzymes with zinc-dependent HDAC activity, and mitochondrial or nuclear sirtuins with NAD⁺-dependent activity [1]. Hdac1 is a class I HDAC, which, together with Hdac2, forms homo- or heterodimers in various transcriptional multiprotein regulators such as NuRD, Sin3A and CoREST [11,12]. *Hdac1* deficiency in mice leads to embryonic death and cell proliferation defects correlating with increased levels of the cyclin-dependent kinase inhibitor p21 [13,14]. Tissue-specific ablation of both *Hdac1* and *Hdac2* leads to differentiation defects in many organs, including the brain [15], the skin [16] and the intestine [17]. Hdac1 represses or activates both global and specific gene expression programs. For example, while Hdac1 acts as a co-activator for glucocorticoid-dependent gene regulation [18], Hdac1 is considered a negative regulator of NF- κ B-dependent transcriptional inflammatory responses by deacetylating the p65 subunit [19]. Hdac1 is associated mostly with active genes and may allow multiple rounds of transcription by clearing promoters of acetylated histone marks [20]. Finally, we have recently shown that Hdac1 may play an important role in establishing and maintaining defined ranges of IL-1 β -dependent inflammatory gene expression in intestinal epithelial cells (IEC) [21].

We have recently shown that Hdac1 reduction by continuous expression of specific shRNAs against Hdac1 reduces proliferation

* Corresponding author. Fax: +1 (819) 820 6831.

E-mail address: Claude.Asselin@USherbrooke.ca (C. Asselin).

and decreases saturation density of non-transformed IEC [21]. Interestingly, this growth defect was not associated with increased expression of cyclin-dependent kinase inhibitors usually augmented in response to HDAC inhibitors or to specific HDAC isoform siRNA-mediated depletion in tumour cell lines [22]. In this study, we provide evidence that Hdac1 reduction indirectly alters cell proliferation by compromising metabolic pathways essential for cell growth. Indeed, Hdac1 depletion leads to modified cell responses to metabolites and oxidative stresses, correlating with the induction of the AMPK signalling pathway and mitochondrial biogenesis. Reduction in acetyl group availability, caused by Hdac1 depletion, may well lead indirectly to metabolic pathway disruption, explaining the severe growth inhibition effect.

2. Materials and methods

2.1. Cell culture

Non-transformed and undifferentiated IEC-6 cells are derived from rat intestinal crypts (CRL-1592, ATCC) [23]. Cells were grown in Dulbecco's modified Eagle medium (DMEM) with 5% fetal bovine serum (FBS). Confluent shCtrl and shHDAC1 IEC-6 cells were cultured in medium without or with 5% FBS and glucose, in normal medium without or with citrate (10 mM) or acetate (10 mM) (Sigma–Aldrich). In some experiments, cells were treated with 5 μ M of the class I inhibitor MS-275 (Cayman), 250 μ M H₂O₂, 500 μ M of the AMPK activator AICAR (Cayman) or 10 μ M AMPK inhibitor compound C (Biovision).

2.2. Retroviral infection

ShCtrl and shHDAC1 cell lines were obtained after puromycin selection of IEC-6 cells with lentiviral shRNA control (SHC002V) or MISSION shRNA HDAC1 (TRCN0000039402) particles (Sigma–Aldrich). This particular shRNA, and the corresponding cell clones, was selected out of three shRNA constructs for Hdac1 reduction levels and growth inhibitory properties [21].

2.3. Western blot analysis

ShCtrl and shHDAC1 IEC-6 cells were resuspended in Laemmli buffer [24], to obtain total cell protein extracts. Nuclei were prepared as before [25,26] and resuspended in Laemmli buffer. Protein concentrations were determined by the BCA method (Thermo Scientific). Proteins loaded on a 6%, 10% or 15% SDS–polyacrylamide gel were electroblotted on a PVDF membrane (Roche). Membranes were incubated 1 h at room temperature, with the following primary antibodies: rabbit anti-Hdac1 (Abcam Inc.); murine anti-actin (EMD Millipore); rabbit anti-histone H3ac and anti-histone H4ac (EMD Millipore); rabbit anti-H3K9ac, -H4K5ac and -H3K56ac (Cell Signalling); goat anti-H4K16ac (Epigentek); rabbit anti-Sod2 (GeneTex); rabbit anti-phospho-AMPK (Thr172), -AMPK, -phosphoacetyl-CoA carboxylase (ACC) (Ser79) (Cell Signalling) [25,26]. Immune complexes were detected with Amersham ECL™ Western blotting detection reagents (GE Healthcare), according to the manufacturer's instructions. Ponceau Red staining was used to detect relative amounts of histones in nuclear extracts. Results are representative of three independent experiments. Additional information about the antibodies used is included in Table S1.

2.4. SILAC labelling, quantification and bioinformatic analysis

Quantitative analysis of protein content was performed after stable isotope labelling with amino acids (SILAC). ShCtrl and shHDAC1 IEC-6 cells were grown in DMEM without arginine and

lysine, supplemented with 5% FBS dialyzed with a cut-off of 10kDa (Life Technologies). Arginine and lysine were added in either light (Arg0, Lys0; Sigma–Aldrich) or heavy isotopes (Arg10, Lys8; Cambridge Isotope Lab) to a final concentration of 28 μ g/ml arginine and 49 μ g/ml lysine, respectively for shCtrl and shHDAC1 IEC-6 cells, during six passages. Whole cell lysates from triplicates of each condition were mixed, subjected to detergent removal, alkylation and trypsin digestion. Digested peptides were used for liquid chromatography–tandem mass spectrometry, data analysis with the MaxQuant program (version 1.1.1.14) and peptide identification with the Andromeda database, as done before [27]. Proteins with shHDAC1 over shCtrl ratios of more than 1.5-fold and less than 0.75-fold were selected for classification according to their gene Ontology biological processes, with the Ingenuity pathway database (<http://www.ingenuity.com>). The mass spectrometry proteomics data have been deposited to the ProteomeXchange Consortium (<http://proteomecentral.proteomexchange.org>) via the PRIDE Partner repository.

2.5. Cell viability measurement

To determine cell viability, fifty thousand shCtrl and shHDAC1 IEC-6 cells were plated in each well. 24 h later, the medium was replaced by medium without or with serum and glucose, or H₂O₂. The next day, 50 μ l of MTT (3-(4,5-dimethylthiazol-2-yl)-2,5-diphenyltetrazolium bromide, 0.5 mg/ml) (Sigma–Aldrich) were added to each well for 2 h at 37 °C. The culture medium was removed before adding 100 μ l of acid-isopropanol solution to solubilise water-insoluble formazan crystals. Optical density was determined on a Versamax ELISA microplate reader at 550 nm (Molecular Devices). Results are expressed as the mean \pm S.E.M. Statistical significance was determined by performing one-way ANOVA. Results are representative of three independent experiments.

2.6. Reactive oxygen species (ROS) measurement

ROS production was measured with the DCFDA Cellular ROS Detection Assay Kit (Abcam) in a 96-well microplate. Ten thousand shCtrl and shHDAC1 IEC-6 cells were plated in each well. After 24 h, cells were incubated in normal medium supplemented with 25 μ M of 2',7'-dichlorofluorescein diacetate (DCFDA) at 37 °C for 45 min. After washing, cells were incubated for 3 h at 37 °C, in normal medium without or with 500 μ M H₂O₂ freshly prepared. ROS concentrations were determined in a microplate reader at a 485 nm excitation wavelength and a 535 nm emission wavelength. Results are expressed as the mean \pm S.E.M. Statistical significance was determined by performing one-way ANOVA. Results are representative of three independent experiments.

2.7. ATP assays

Ten thousand shCtrl and shHDAC1 IEC-6 cells were plated in each well. The following day, an equal volume of ATP assay solution (PhosphoWorks Luminometric ATP Assay Kit *Study Glow*, AAT Bioquest) was added to each well for 10 min at room temperature. ATP concentration was determined by reading flash luminescence for 1 s with an Orion Microplate Luminometer (Berthold Technologies). The experiment was done three times in triplicate. Results are expressed as the mean \pm S.E.M. Statistical significance was determined by performing unpaired *t* tests.

2.8. Mitochondria labelling

Mitochondria were labelled with the Cell Navigator™ Mitochondrion Staining Kit (AAT Bioquest). Ten thousand cells were placed in a LAB-TEK (Thermo Fisher Scientific). After 24 h, cells were

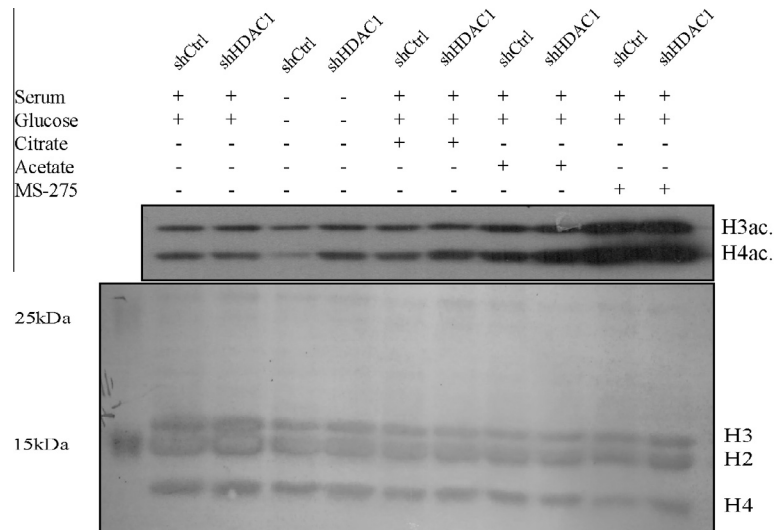


Fig. 1. Hdac1 depletion affects IEC-6 cell metabolite-dependent histone acetylation. IEC-6 shCtrl and shHDAC1 cells were cultured for 24 h in normal medium, in medium without serum and glucose, in normal medium with added citrate, acetate and class I HDAC inhibitor MS-275. Nuclear extracts were resuspended in Laemmli buffer. Nuclear proteins were separated on a 15% SDS-PAGE gel and transferred to PVDF membranes for Western blot analysis of total acetylated H3 (H3 ac.) and acetylated H4 (H4 ac.). Ponceau Red staining was used to detect relative amounts of histones in nuclear extracts. Experiments were performed in triplicate and results from one representative blot are shown.

treated with a combination of Mitolite™ Green and Live Cell Staining Buffers for 4 h at 37 °C. The buffer was then replaced with PBS. Mitochondria were observed with an Inverse Zeiss Fluorescence Microscope (Carl Zeiss) at a 40× magnification and FITC filter set of Ex/Em = 485/525 nm, with 500 ms time of exposition. Images were generated with the AxioVision software (Carl Zeiss).

2.9. qPCR analysis

2 ng of cDNAs, prepared from shCtrl and shHDAC1 IEC-6 cell mRNAs, were used for qPCR using the RT² SYBR Green ROX qPCR Master Mix (Qiagen), and oligonucleotides against selected mitochondrial nuclear-expressed genes, namely Tfb2m, Tfam, Aldh2, Idh2 and Atp5O (Table S1). Relative quantification was assessed by Tbp amplification. Ten min incubation at 95 °C was followed by 40 cycles of 10 s at 95 °C, 10 s at 60 °C and 20 s at 72 °C. Results are expressed as the mean ± S.E.M. Statistical significance was determined by performing unpaired *t* tests. Results are representative of two independent experiments.

3. Results and discussion

We have previously shown that shRNA-dependent Hdac1 reduction (21, Fig. S1) led to a cyclin-dependent kinase inhibitor-independent decrease in IEC-6 cell proliferation [21]. In order to determine how Hdac1 depletion affected IEC-6 cell growth, we first verified the impact of Hdac1 depletion on global histone acetylation in IEC-6 cells. ShCtrl and shHDAC1 cells were grown in medium without glucose and serum, in medium supplemented with acetyl-CoA donors citrate and acetate, or in medium containing the HDAC class I Hdac1, Hdac2 and Hdac3 deacetylase inhibitor MS-275. As shown by Wellen et al. [10], absence of glucose and serum resulted in decreased levels of acetylated histone H3 and H4 in shCtrl cells (Fig. 1) and of site-specific acetylated marks H3K9ac, H3K56ac, H4K5ac and H4K16ac (Fig. S2). In contrast, histone acetylated levels were maintained in shHDAC1 cells, even in the absence of glucose and serum (Figs. 1 and S2). This indicates that Hdac1 plays an important role in the turnover of histone acetyl groups in response to metabolic disturbances. Acetate

Table 1

Pathway analysis of decreased and induced proteins in shHDAC1 depleted IEC-6 cells. Hdac1 depletion leads to altered expression of mitochondrial and mTOR pathway proteins. More than 1.5-fold or less than 0.75-fold induced or repressed proteins in shHDAC1 depleted IEC-6 cells were selected for the analysis. Pathway analysis of decreased and induced proteins in shHDAC1 depleted IEC-6 cells was done according to biological processes identified with the Ingenuity pathway database. The top canonical pathway induced and the top canonical pathway decreased, are indicated.

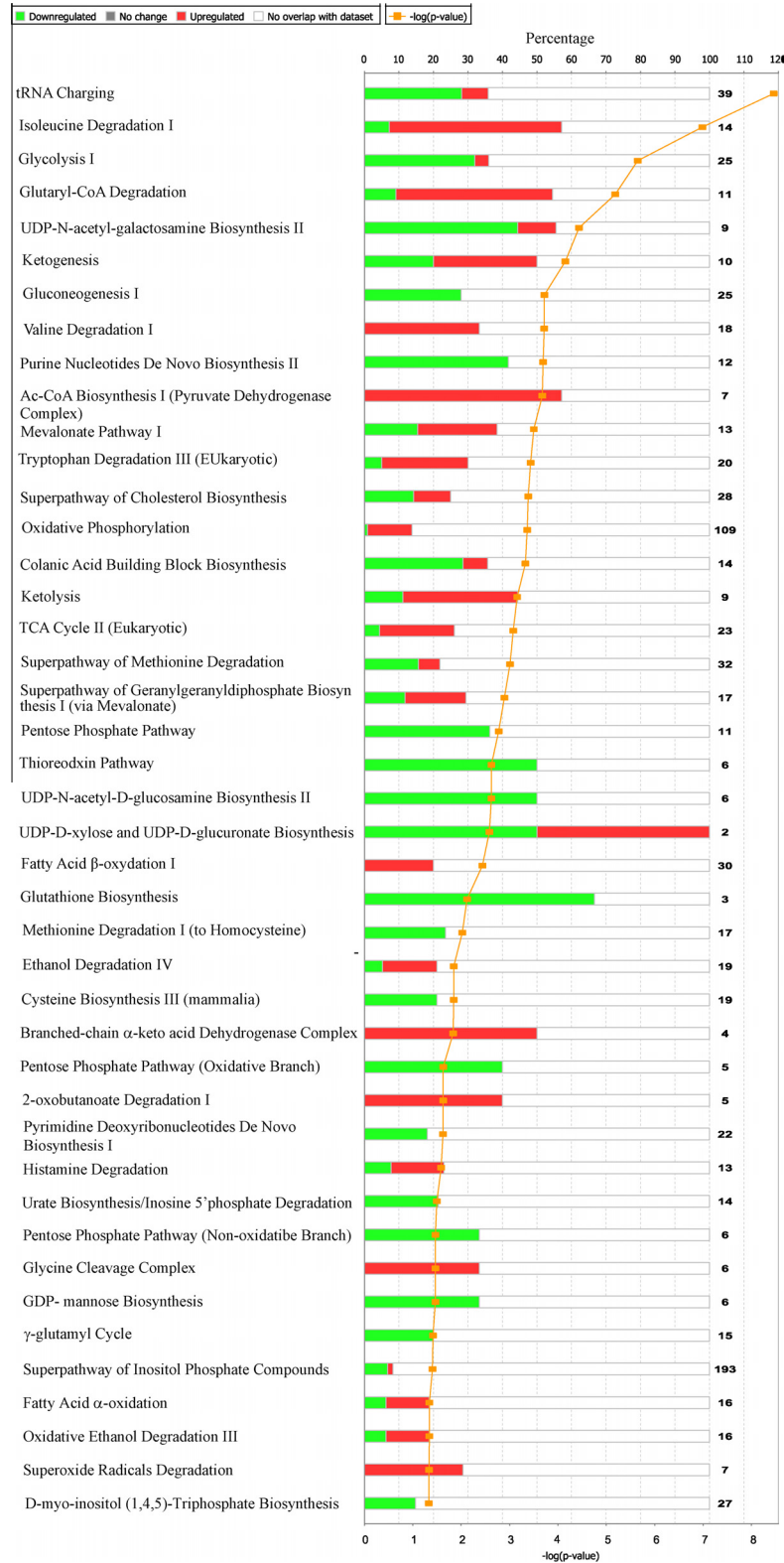
Name	P-value	Ratio
Top canonical pathway induced		
Mitochondrial dysfunction	6,96E-17	27/215
Isoleucine degradation	8,08E-09	07/30
Oxidative phosphorylation	4,50E-08	14/120
Valine degradation I	1,08E-06	06/35
Top canonical pathway decreased		
EIF2 signalling	2,68E-19	37/201
Regulation of eIF4 and p70S6K signalling	2,39E-13	27/175
mTOR signalling	5,92E-10	26/213
Protein ubiquitination pathway	4,35E-09	29/270

addition led to stronger increases in histone acetylation, notably of H4, in shHDAC1 cells as compared to shCtrl cells grown in normal medium (Figs. 1 and S2). This suggests that Hdac1 depletion increases steady-state levels of histone acetylation resulting from acetyl-CoA donor addition, by decreasing turnover efficiency. However, other class I enzymes are involved in this turnover, as MS-275 led to increased histone acetylated levels in both shCtrl and shHDAC1 cells (Figs. 1 and S2). Thus, these data suggest that Hdac1 regulates global histone acetylation levels in IEC-6 cells. In addition, acetylated histone levels are more increased in the absence of Hdac1, as opposed to control cells, in conditions when acetyl-CoA production is increased. Thus, Hdac1 depletion, by reducing the availability of acetyl groups for metabolic reactions, could impact on cell growth by altering metabolic responses in IEC-6 cells.

To determine the phenotypic changes resulting from Hdac1 depletion, we analysed the proteome of shCtrl and shHDAC1 IEC-6 cells by differential labelling with light and heavy isotopes of arginine and lysine, with the SILAC method [27,28]. We separately analysed upregulated and downregulated proteins in shHDAC1

Table 2

Metabolic pathway disturbances in shHDAC1 depleted IEC-6 cells. Metabolic pathway alterations resulting from Hdac1 reduction in IEC-6 cells are represented as a bar graph with up and downregulated pathways of metabolic processes, such as respectively, degradation pathways and synthesis processes. Pathway analysis of decreased and induced proteins was done according to biological processes identified with the Ingenuity pathway database.



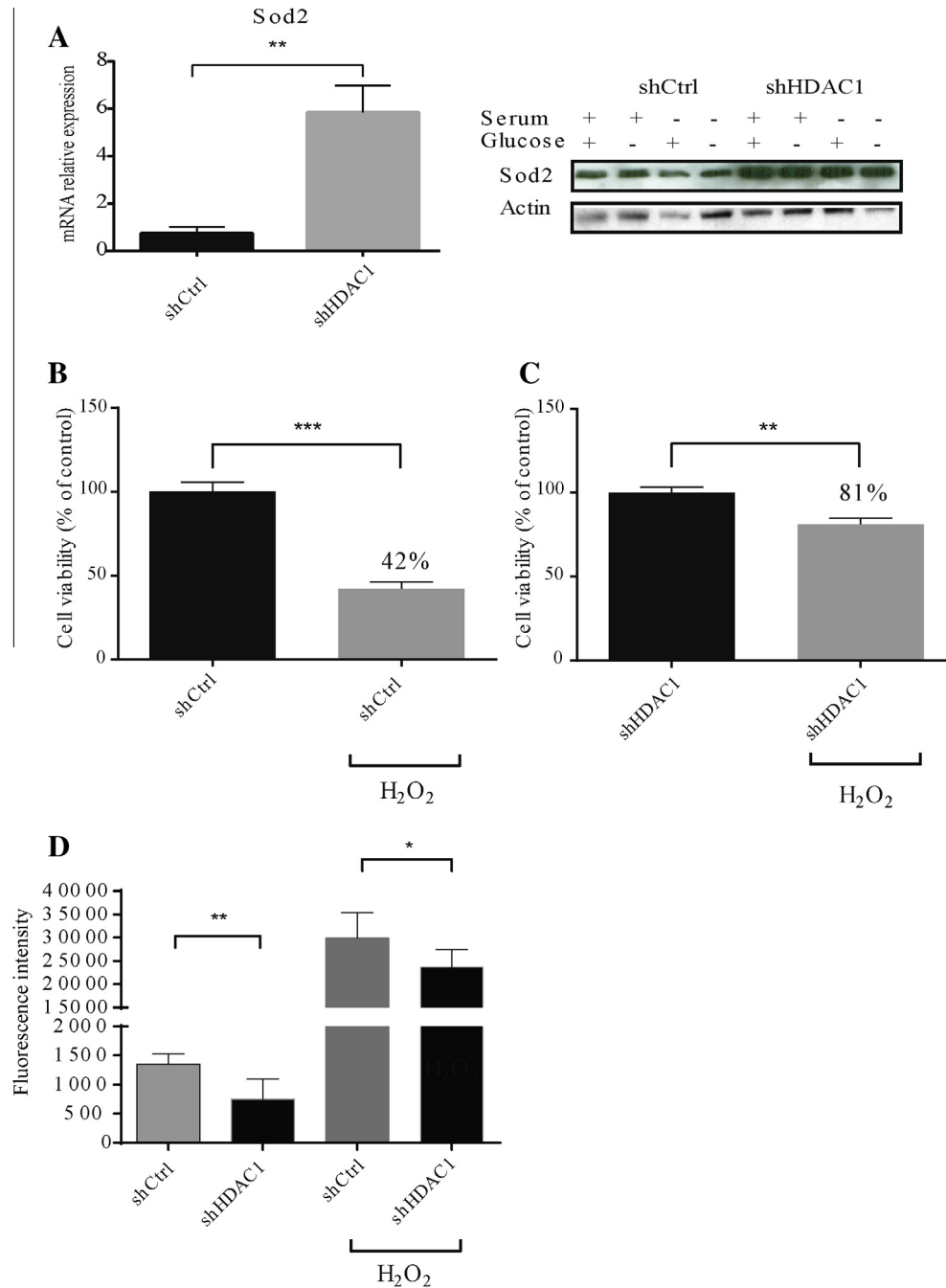


Fig. 2. (A–C) Hdac1 depletion leads to altered IEC-6 cell responses to oxidative stress. (A) Expression levels of Sod2 and Pbgd, as a loading control, were determined by quantitative PCR of cDNAs obtained from total shCtrl and shHDAC1 IEC-6 RNAs. Results represent the mean \pm S.E.M. (** $P \leq 0.01$). Statistical significance was determined by unpaired *t* tests (left panel). ShCtrl and shHDAC1 IEC-6 cells were cultured for 24 h in medium with or without serum and glucose. Cells were resuspended in Laemmli buffer. Total proteins were analysed for Sod2 and actin, as a protein loading control, by Western blot. Experiments were performed in triplicate and results from one representative experiment are shown (right panel). (B and C) ShCtrl (B) and shHDAC1 (C) IEC-6 cells in 24-well plates were cultured for 24 h in medium with 250 μ M hydrogen peroxide. Cells were labelled for 2 h with MTT to evaluate cell viability. Graphics were created with GraphPad Prism software and statistics determined by ANOVA test (** $P \leq 0.01$; *** $P \leq 0.005$). The experiment was performed in triplicate and results of a representative experiment are shown. (D) Hdac1 depletion leads to reduction of reactive oxygen radical production. ShCtrl and shHDAC1 IEC-6 cells in 24-well plates were treated with DCFDA for 45 min, before adding 500 μ M hydrogen peroxide for 3 h. Relative amounts of free radicals were measured by spectrofluorimetry. Graphics were created with GraphPad Prism software and statistics determined by ANOVA test (* $P \leq 0.05$; ** $P \leq 0.01$). The experiment was performed in triplicate and the results of a representative experiment are shown.

cells and compared to shCtrl cells. Surprisingly, we found that the main altered categories were related to energy metabolism. Indeed, the Top induced canonical pathways included Mitochondrial Dysfunction, Isoleucine Valine Degradation and Oxidative Phosphorylation (P -value from $6.96E-17$ to $4.5E-08$) (Table 1).

The Top decreased canonical pathways were related to protein synthesis and cell energy sensing, and included EIF2 Signalling, Regulation of eIF4 and p70S6K Signalling, mTOR Signalling and Protein Ubiquitination Pathway (P -value from $2.68E-19$ to $4.3E-09$). Proteins increased more than 1.5-fold in the

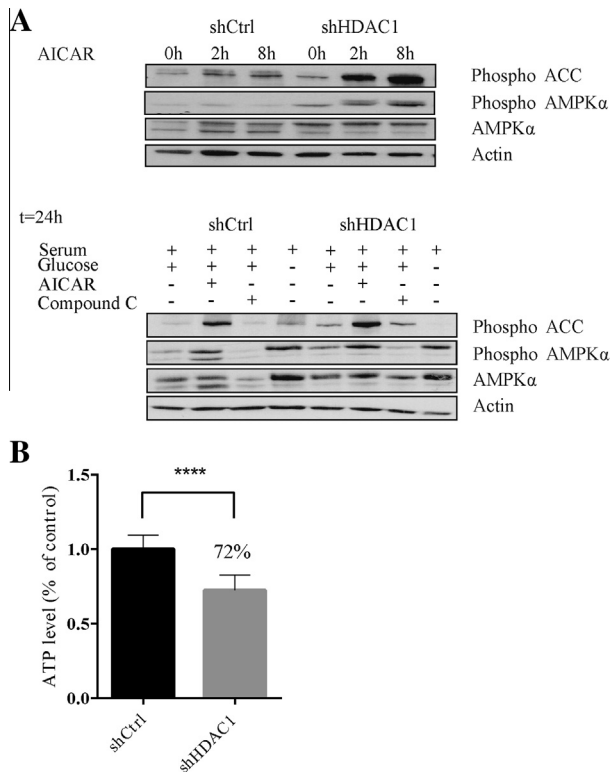


Fig. 3. Hdac1 depletion leads to increases of basal and induced levels of AMPK phosphorylation correlating with decreased ATP production. (A) ShCtrl and shHDAC1 IEC-6 cells were cultured for 2 or 8 h in medium containing AICAR (upper panel) or for 24 h in medium with or without serum and glucose, or in complete medium containing AICAR or compound C (lower panel). Cells were resuspended in Laemmli buffer. Total proteins were analysed for phospho-ACC, phospho-AMPK α , AMPK α and actin, as a protein loading control, by Western blot. Experiments were performed in triplicate and results from one representative experiment are shown. (B) Ten thousand shCtrl and shHDAC1 IEC-6 cells were grown in 96-well-plates and ATP was measured with a Luciferase ATP assay kit. Statistical significance was determined by unpaired *t* tests (**** $P \leq 0.001$).

Mitochondrial Dysfunction pathway and proteins decreased more than 1.5-fold in the Protein Synthesis pathway are listed in Table S3. Closer analysis of the altered metabolic pathways showed downregulation of ARNt charging, correlating with increased amino acid degradation pathways, including valine and isoleucine (Table 2). In addition, lipid β -oxidation and acetyl-CoA biosynthesis pathways were increased. This suggests that Hdac1 depletion leads to a reduction of normal metabolic processes and to induction of degradation pathways to supply metabolites necessary to ensure cell viability. Again, this coincides with altered mitochondrial function and mTOR energy sensing signalling upon Hdac1 depletion. This is intriguing since the Hdac1 deacetylase is mostly a nuclear protein, with predominantly nuclear substrates [11,29].

As proteome analysis revealed an increase of proteins associated with mitochondria and oxidative responses, we first verified the expression of superoxide dismutase 2 (Sod2), an antioxidant protein with manganese-dependent activity [30], whose protein expression is increased 7.4-fold in shHDAC1 cells (Table S3). QPCR analysis confirmed induced expression at the mRNA level (Fig. 2A). In addition, basal Sod2 protein levels were increased in shHDAC1 cells, as opposed to shCtrl cells, independently of energy-deficient cell culture conditions (Fig. 2A). We then determined whether Hdac1 reduction affected IEC-6 viability in medium depleted of glucose and serum, by MTT assay. Hdac1 depleted cells

displayed increased viability. Indeed, cell viability was reduced by 23% for shHDAC1 cells ($P < 0.05$), instead of 46% for shCtrl cells ($P < 0.0001$). The same was observed in response to the oxidant H₂O₂: shCtrl cells were twofold more sensitive than shHDAC1 cells to oxidative stress induced by H₂O₂ (Fig. 2B and C). We then measured the relative amounts of reactive oxygen species (ROS) after loading cells with DCFDA, whose accumulation correlates with ROS levels. ShHDAC1 cells displayed decreased basal as well as H₂O₂-mediated ROS levels, as opposed to shCtrl cells (Fig. 2D).

Proteomic analysis also revealed possible perturbations in cell energy levels. To determine this, we assessed the activity of AMPK, a major energy cell sensor of AMP to ATP concentrations [31]. AMPK is allosterically activated by AMP, leading to promotion of ATP-generating metabolic reactions and reduction of ATP-consuming anabolic pathways regulated in part by mTOR. ShHDAC1 cells displayed increased basal activation of AMPK α , as assessed by Western blot analysis with an antibody against a phosphorylated form, as well as increased phosphorylation of the AMPK α substrate ACC (Fig. 3A).

While the AMPK inhibitor compound C reduced AMPK α phosphorylation in both cell types, treatment with the AMPK activator AICAR led to increased AMPK α activation in shHDAC1 and shCtrl cells. Moreover, shHDAC1 cells produced less ATP, as opposed to shCtrl cells, suggesting an increase in the levels of the AMPK α activator, namely AMP (Fig. 3B). These results suggest that Hdac1 depletion leads to metabolic alterations resulting in restriction of energy metabolism and sustained activation of AMPK α , a negative regulator of the mTOR pathway. As our proteome analysis suggested mitochondrial alterations and as AMPK α regulation of mitochondrial biogenesis may be related in part to constitutive AMPK activation [32], we verified mitochondrial content by fluorescent labelling. Microscopy analysis shows that Hdac1 depleted cells were enlarged, with bigger nuclei, and contained increased numbers of mitochondria (Fig. 4A). Increased mRNA expression of genes associated with mitochondria, such as Tf2m, Aldh2, Idh2 and Atp50, as assessed by qPCR, confirmed increased mitochondrial biogenesis (Fig. 4B).

It has been proposed that changes in epigenetic regulator activities, by reducing the availability of cellular metabolites, could influence metabolic pathways and cell homeostasis, as well as gene expression patterns [33]. We show here that depletion in a nuclear deacetylase, namely Hdac1, in intestinal epithelial cells, results in metabolic changes associated with ATP energy source depletion, with altered responses to metabolic substrates and oxidative stresses, and impaired increased activation of AMPK α , accompanied with mitochondrial biogenesis. These observations are supported by recent studies, one showing that depletion of Sin3A, which is a component of a Hdac1-containing co-repressor complex [12], alters mitochondrial activity in *Drosophila* cells [34], the other showing that class I HDAC inhibitors increase mitochondrial biogenesis in cultured myotubes and adipocytes [35]. We suggest that the absence of nuclear Hdac1 may indirectly alter cellular metabolism and energy levels by restricting the availability of acetyl groups for acetyl-CoA, or other metabolite, production, therefore decreasing their availability for metabolic reactions. Indeed, limited removal of the acetyl groups on histones occurs in the absence of Hdac1, even in conditions lowering the acetylated mark, such as in low glucose conditions, as reported by Wellen et al. [10]. Increased retention of the acetyl group on histones could lead to decreased ATP production, increased AMPK activation and mitochondrial biogenesis, thereby favoring the use of other energy sources. Our results suggest that Hdac1 depletion may alter metabolic pathways, leading to different responses to metabolic changes, and affecting in part the oxidative response.

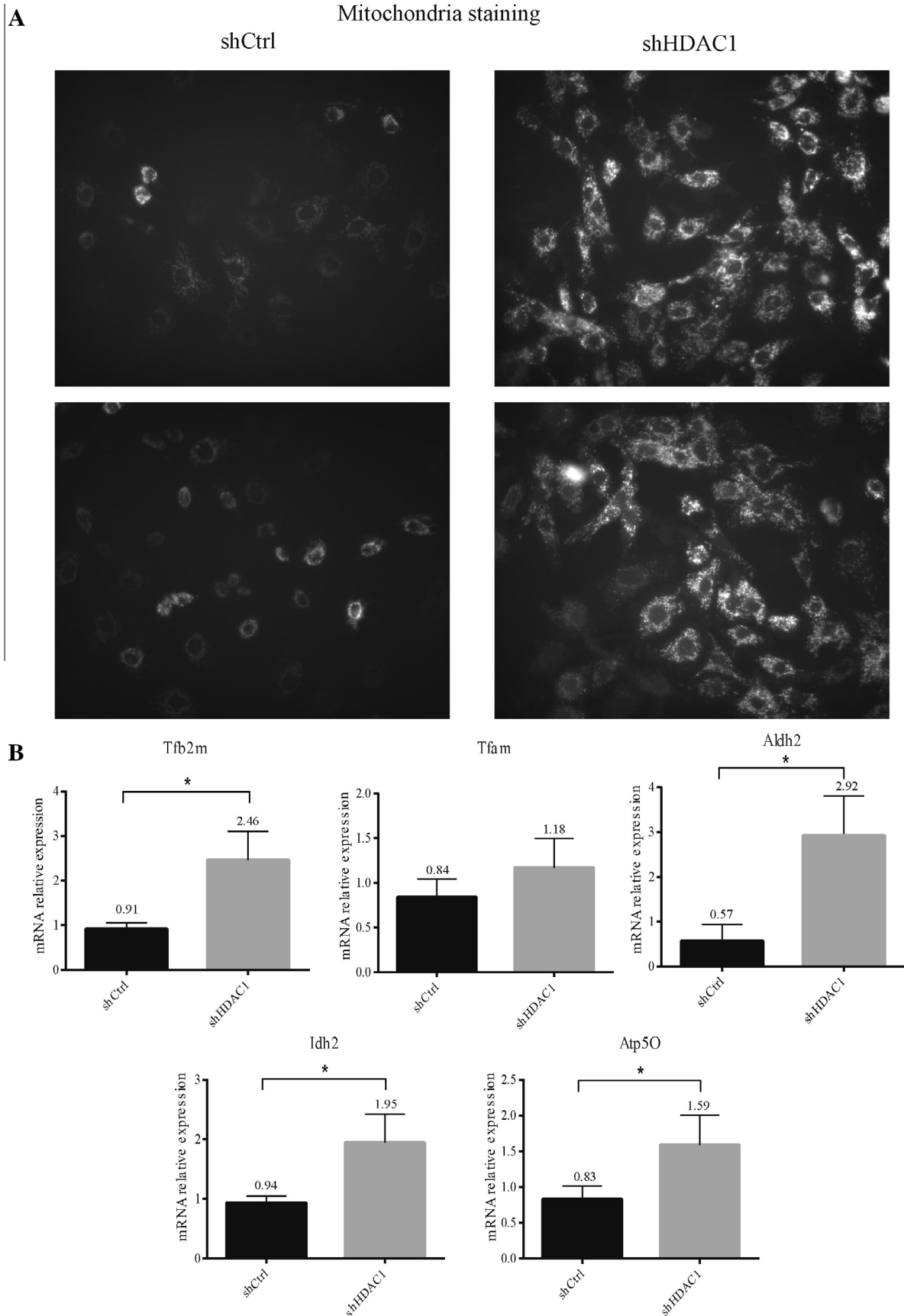


Fig. 4. Hdac1 depletion leads to increased mitochondrial biogenesis. (A) Ten thousand cells plated in a LAB-TEK were treated with a combination of Mitolite™ Green and Live Cell Staining Buffers to stain mitochondria. Cell mitochondria were observed with an Inverse Zeiss Fluorescence Microscope at a 40× magnification and FITC filter set of Ex/Em = 485/525 nm, with 500 ms time of exposition. Images were generated with the AxioVision software. (B) Total RNAs were isolated from shCtrl and shHDAC1 IEC-6 cells. Relative expression levels of selected mitochondria-associated genes, namely Tfb2m, Tfam, Aldh2, Atp5O and Idh2, were verified by quantitative PCR, with Tbp as a loading control. Results represent the mean ± S.E.M. ($P < 0.05$). Statistical significance was determined by unpaired *t* tests.

Author contributions

AG, NT, FMB, FB, CA: conceived and designed the experiments. AG, NT: performed the experiments. AG, NT, FMB, FB, CA: analysed the data. AG, FB, CA: wrote the paper. All authors read and approved the final manuscript.

Acknowledgements

This research was supported by a grant from Crohn's and Colitis Canada. Claude Asselin, François-Michel Boisvert and François Boudreau are members of the Fonds de recherche du Quebec-Sante-funded CR-CHUS.

Appendix A. Supplementary data

Supplementary data associated with this article can be found, in the online version, at <http://dx.doi.org/10.1016/j.febslet.2015.08.009>.

References

- [1] Yang, X.J. and Seto, E. (2008) The Rpd3/Hda1 family of lysine deacetylases: from bacteria and yeast to mice and men. *Nat. Rev. Mol. Cell Biol.* 9, 206–218.
- [2] Choudhary, C., Kumar, C., Gnad, F., Nielsen, M.L., Rehman, M., Walther, T.C., Olsen, J.V. and Mann, M. (2009) Lysine acetylation targets protein complexes and co-regulates major cellular functions. *Science* 325, 834–840.
- [3] Patel, J., Pathak, R.R. and Mujtaba, S. (2011) The biology of lysine acetylation integrates transcriptional programming and metabolism. *Nutr. Metab. (Lond.)* 8, 12.
- [4] Choudhary, C., Weinert, B.T., Nishida, Y., Verdin, E. and Mann, M. (2014) The growing landscape of lysine acetylation links metabolism and cell signalling. *Nat. Rev. Mol. Cell Biol.* 15, 536–550.
- [5] Hait, N.C. et al. (2009) Regulation of histone acetylation in the nucleus by sphingosine-1-phosphate. *Science* 325, 1254–1257.
- [6] Shimazu, T. et al. (2013) Suppression of oxidative stress by beta-hydroxybutyrate, an endogenous histone deacetylase inhibitor. *Science* 339, 211–214.
- [7] Newman, J.C. and Verdin, E. (2014) Beta-hydroxybutyrate: much more than a metabolite. *Diabetes Res. Clin. Pract.* 106, 173–181.
- [8] Huang, H. et al. (2012) L-carnitine is an endogenous HDAC inhibitor selectively inhibiting cancer cell growth in vivo and in vitro. *PLoS One* 7, e49062.
- [9] Wellen, K.E. and Thompson, C.B. (2012) A two-way street: reciprocal regulation of metabolism and signalling. *Nat. Rev. Mol. Cell Biol.* 13, 270–276.
- [10] Wellen, K.E., Hatzivassiliou, G., Sachdeva, U.M., Bui, T.V., Cross, J.R. and Thompson, C.B. (2009) ATP-citrate lyase links cellular metabolism to histone acetylation. *Science* 324, 1076–1080.
- [11] Moser, M.A., Hagelkruys, A. and Seiser, C. (2014) Transcription and beyond: the role of mammalian class I lysine deacetylases. *Chromosoma* 123, 67–78.
- [12] McDonel, P., Costello, I. and Hendrich, B. (2009) Keeping things quiet: roles of NuRD and Sin3 co-repressor complexes during mammalian development. *Int. J. Biochem. Cell Biol.* 41, 108–116.
- [13] Zupkovitz, G. et al. (2010) The cyclin-dependent kinase inhibitor p21 is a crucial target for histone deacetylase 1 as a regulator of cellular proliferation. *Mol. Cell Biol.* 30, 1171–1181.
- [14] Lager, G. et al. (2002) Essential function of histone deacetylase 1 in proliferation control and CDK inhibitor repression. *EMBO J.* 21, 2672–2681.
- [15] Hagelkruys, A. et al. (2014) A single allele of Hdac2 but not Hdac1 is sufficient for normal mouse brain development in the absence of its paralog. *Development* 141, 604–616.
- [16] Winter, M. et al. (2013) Divergent roles of HDAC1 and HDAC2 in the regulation of epidermal development and tumorigenesis. *EMBO J.* 32, 3176–3191.
- [17] Turgeon, N., Blais, M., Gagne, J.M., Tardif, V., Boudreau, F., Perreault, N. and Asselin, C. (2013) HDAC1 and HDAC2 restrain the intestinal inflammatory response by regulating intestinal epithelial cell differentiation. *PLoS One* 8, e73785.
- [18] Qiu, Y. et al. (2006) HDAC1 acetylation is linked to progressive modulation of steroid receptor-induced gene transcription. *Mol. Cell* 22, 669–679.
- [19] Ghizzoni, M., Haisma, H.J., Maarsingh, H. and Dekker, F.J. (2011) Histone acetyltransferases are crucial regulators in NF-kappaB mediated inflammation. *Drug Discov. Today* 16, 504–511.
- [20] Wang, Z., Zang, C., Cui, K., Schones, D.E., Barski, A., Peng, W. and Zhao, K. (2009) Genome-wide mapping of HATs and HDACs reveals distinct functions in active and inactive genes. *Cell* 138, 1019–1031.
- [21] Gonneaud, A., Gagne, J.M., Turgeon, N. and Asselin, C. (2014) The histone deacetylase Hdac1 regulates inflammatory signalling in intestinal epithelial cells. *J. Inflamm. (Lond.)* 11, 43.
- [22] Ocker, M. and Schneider-Stock, R. (2007) Histone deacetylase inhibitors: signalling towards p21cip1/waf1. *Int. J. Biochem. Cell Biol.* 39, 1367–1374.
- [23] Quaroni, A. and May, R.J. (1980) Establishment and characterization of intestinal epithelial cell cultures. *Methods Cell Biol.* 21B, 403–427.
- [24] Gheorghiu, I., Deschenes, C., Blais, M., Boudreau, F., Rivard, N. and Asselin, C. (2001) Role of specific CCAAT/enhancer-binding protein isoforms in intestinal epithelial cells. *J. Biol. Chem.* 276, 44331–44337.
- [25] Turgeon, N., Valiquette, C., Blais, M., Routhier, S., Seidman, E.G. and Asselin, C. (2008) Regulation of C/EBPdelta-dependent transactivation by histone deacetylases in intestinal epithelial cells. *J. Cell. Biochem.* 103, 1573–1583.
- [26] Turgeon, N., Blais, M., Delabre, J.F. and Asselin, C. (2013) The histone H3K27 methylation mark regulates intestinal epithelial cell density-dependent proliferation and the inflammatory response. *J. Cell. Biochem.* 114, 1203–1215.
- [27] Boisvert, F.M., Ahmad, Y., Gierlinski, M., Charriere, F., Lamont, D., Scott, M., Barton, G. and Lamond, A.I. (2012) A quantitative spatial proteomics analysis of proteome turnover in human cells. *Mol. Cell. Proteomics* 11 (M111), 011429.
- [28] Drissi, R., Dubois, M.L. and Boisvert, F.M. (2013) Proteomics methods for subcellular proteome analysis. *FEBS J.* 280, 5626–5634.
- [29] Kelly, R.D. and Cowley, S.M. (2013) The physiological roles of histone deacetylase (HDAC) 1 and 2: complex co-stars with multiple leading parts. *Biochem. Soc. Trans.* 41, 741–749.
- [30] Flynn, J.M. and Melov, S. (2013) SOD2 in mitochondrial dysfunction and neurodegeneration. *Free Radic. Biol. Med.* 62, 4–12.
- [31] Hardie, D.G., Ross, F.A. and Hawley, S.A. (2012) AMPK: a nutrient and energy sensor that maintains energy homeostasis. *Nat. Rev. Mol. Cell Biol.* 13, 251–262.
- [32] Sullivan, L.B. and Chandel, N.S. (2014) Mitochondrial metabolism in TCA cycle mutant cancer cells. *Cell Cycle* 13, 347–348.
- [33] Martinez-Pastor, B., Cosentino, C. and Mostoslavsky, R. (2013) A tale of metabolites: the cross-talk between chromatin and energy metabolism. *Cancer Discov.* 3, 497–501.
- [34] Barnes, V.L., Strunk, B.S., Lee, I., Huttemann, M. and Pile, L.A. (2010) Loss of the SIN3 transcriptional corepressor results in aberrant mitochondrial function. *BMC Biochem.* 11, 26.
- [35] Galmozzi, A. et al. (2013) Inhibition of class I histone deacetylases unveils a mitochondrial signature and enhances oxidative metabolism in skeletal muscle and adipose tissue. *Diabetes* 62, 732–742.